



J. Serb. Chem. Soc. 88 (4) 367–379 (2023)
JSCS–5632

Binding interactions of actinomycin D anticancer drug with bile salts micelles

ANA MARIA TOADER, IZABELLA DASCALU, ELENA IONELA NEACSU
and MIRELA ENACHE*

*Institute of Physical Chemistry “Ilie Murgulescu”, Romanian Academy,
Splaiul Independentei 202, Bucharest 060021, Romania*

(Received 2 November 2022, revised 17 January, accepted 25 January 2023)

Abstract: The interactions of actinomycin D (ActD) anticancer drug with two bile salts of different hydrophobicity (sodium cholate (NaC) and sodium deoxycholate (NaDC) and the influence of these bile salts aggregates on the ActD–DNA complex was investigated in 10 mM phosphate buffer (pH 7.4) by UV–Vis spectroscopy (absorption and thermal denaturation). The binding strength of ActD to NaDC is higher than for NaC, and this difference attests stronger hydrophobic interactions between ActD and NaDC micelles. Also, the partition coefficient is significantly higher for NaDC micelles than for NaC micelles, in line with larger aggregates formed by NaDC. The spectral profile of ActD molecules in NaC and NaDC micelles, in comparison with different solvents, implies that ActD molecule experiences a hydrophobic environment in bile salts aggregates. Regarding the influence of NaC and NaDC aggregates on the ActD–DNA complex, it was shown that the presence of both bile salts micelles do not induce the deintercalation of ActD molecules from DNA duplex.

Keywords: binding constant; partition coefficient; deintercalation.

INTRODUCTION

Actinomycin D or dactinomycin (ActD), isolated from *Streptomyces* species, is a well-known antibiotic that exhibits high antitumor and antibacterial activity. ActD is used alone, or in combination with other drugs to treat many tumors, such as Wilms and Ewing tumors, testicular cancer, sarcomas and choriocarcinoma.^{1–3} Structurally, ActD contains a 2-aminophenoxazin-3-one chromophore and two identical cyclic pentapeptide lactones (Fig. 1).

ActD exerts its biological activity *via* the inhibition of transcription by binding DNA at the transcription initiation complex and *via* the prevention of elongation of RNA chain by RNA polymerase.⁴

* Corresponding author. E-mail: enachemir@yahoo.com
<https://doi.org/10.2298/JSC221102004T>

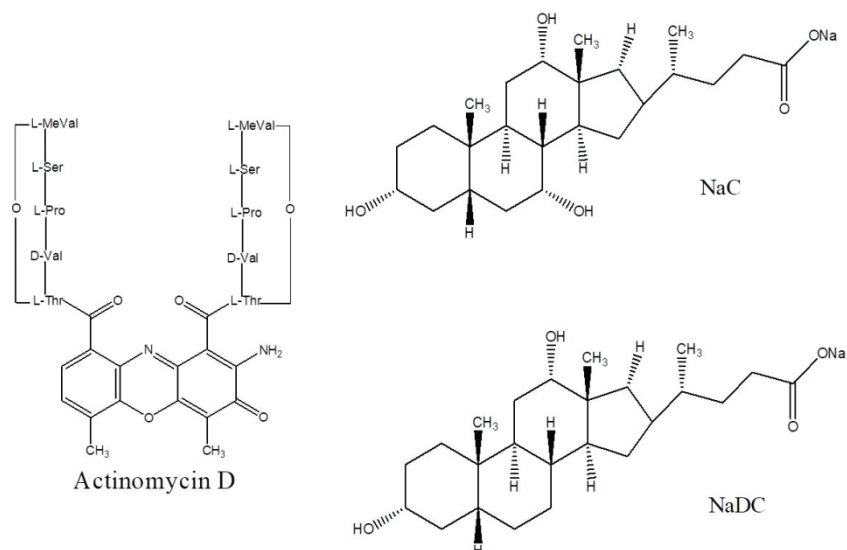


Fig. 1. Molecular structures of ActD, sodium cholate (NaC) and sodium deoxycholate (NaDC).

Bile salts are naturally occurring amphiphilic molecules, synthesized from cholesterol in the liver, deposited in the gall bladder, and then secreted into the small intestine. Unlike conventional surfactants, bile salts have a rigid nonplanar steroidal skeleton with a convex side of hydrophobic groups and a concave side which is made up of hydrophilic polar groups (typically two or three hydroxyl groups). Beside the physiological functions like solubilization and digestion of fats and lipids, hydrolysis of triglycerides, cholesterol elimination from the body,^{5,6} bile salts aggregates play a significant role in pharmaceutical, biochemical and cosmetic fields.^{7,8} Due to their biocompatible and biodegradable nature, there has been a growing interest in using bile salts aggregates as drug carrier vehicles to increase drug transport across various biological barriers such as the blood-brain, nasal, pulmonary and intestinal membranes.⁹ As a result of their particular structure and the rigidity of molecules, bile salts exhibit distinct properties of aggregation in comparison with those of traditional surfactants.¹⁰ Various models have been proposed to explain the uncommon aggregation behaviour of bile salts. The primary and secondary aggregate model proposed by Small *et al.* is the most widely accepted one.^{11–16} According to this model, in the first step the small primary aggregates containing 2 to 10 monomers are formed around the critical micellar concentration (CMC) by the hydrophobic interaction between the convex hydrophobic surfaces of monomers. In the second step at higher concentration of bile salts, the larger secondary aggregates are formed by

the interaction of the primary aggregates *via* the formation of hydrogen bonds between the hydroxyl groups.

Due to the presence of different binding sites, bile salt aggregates are interesting host systems capable to bind both hydrophobic and hydrophilic guest molecules depending on the structure and size of the guests.^{17–20}

Taking into account the intracellular damage caused by reactive oxygen species or reactive radical intermediates generated by the bioreduction of the quinone–imine structure of ActD,²¹ a possible way to overcome these toxic side effects is to use the bile salts aggregates as drug carrier systems. Bearing this in mind and in continuation of our interest in the study of the interaction of drugs with biomimicking assemblies (surfactant and bile salts micelles), in this work we have investigated the interaction of ActD with two different bile salts, sodium cholate (NaC) and sodium deoxycholate (NaDC). NaC and NaDC bile salts contain the same head group ($-\text{CH}_2-\text{CH}_2-\text{COO}^-$) but NaC contains one hydroxyl group more in the hydrophilic surface making NaC more hydrophilic than NaDC. The present paper is divided into two parts: the first part describes the interaction of ActD with NaC and NaDC micelles, and the second part deals with the influence of these bile salts micelles on the ActD–DNA complexes. Spectral (absorption and thermal denaturation) measurements were used to accomplish the proposed aims.

EXPERIMENTAL

Materials

Actinomycin D (98 % purity, ActD), sodium cholate (99 % purity, NaC), sodium deoxycholate (97 % purity, NaDC), deoxyribonucleic acid (DNA) sodium salt from calf thymus, pyrene and other chemicals were purchased from Sigma–Aldrich and employed as received. Experiments were performed in 10 mM phosphate buffer (pH 7.4) and deionized water (Mili-Q water purification system) was used for the preparation of solutions. The concentration of ActD solution was determined using its molar absorption coefficient, $\epsilon = 24450 \text{ M}^{-1} \text{ cm}^{-1}$ at 440 nm.²² DNA stock solution was prepared by dissolving solid DNA in 10 mM phosphate buffer and the exact concentration of DNA solutions was determined by measuring the absorbance at 260 nm and using the molar absorption coefficient $\epsilon = 6600 \text{ M}^{-1} \text{ cm}^{-1}$.

Apparatus and methods

Spectrophotometric measurements were made on a Jasco V-630 spectrophotometer equipped with a Peltier-controlled ETCR-762 model accessory (Jasco Corporation, Tokyo, Japan) using a matched pair of quartz cuvettes with a path length of 1 cm. The absorption spectra of ActD in 10 mM phosphate buffer (pH 7.4) and in the presence of different concentrations of NaC and NaDC were recorded in the wavelength range of 300–600 nm.

For thermal denaturation experiments, the absorbance at 260 nm of DNA solution, ActD–DNA complex and ActD–DNA complex in the presence of bile salts aggregates was measured in the temperature range 20 to 95 °C with heating speed of 1 °C/min. The melting temperature (T_m) was taken as the midpoint of the melting curve. All measurements of T_m were repeated three times and the data presented are average values.

The hyperchromicity (H) of DNA was calculated as:²³

$$H = 100 \frac{A_U - A_L}{A_L} \quad (1)$$

where A_U and A_L are the absorbance of the upper baseline and the absorbance of the lower baseline, respectively.

RESULTS AND DISCUSSION

Binding interaction of actinomycin D with NaC and NaDC micelles

Fig. 2 displays the absorption spectra of ActD in the presence of different increasing NaC (Fig. 2a) and NaDC concentrations (Fig. 2b). In 10 mM phosphate buffer (pH 7.4) ActD presents a broad absorption maxima around 440 nm, including at least three different electronic transitions: one is centred at about 372 nm is localized to a large degree on the benzenoid part of the phenoxazone chromophore; the second one located at about 490 nm is predominantly centred on the quinoid ring and the third transition occurs in the range 425–445 nm is extensively delocalized across the entire chromophore.²⁴ The incremental addition of NaC and NaDC leads to the following spectral behaviour: for bile salts concentrations less than *CMC*, a minor influence on the absorption spectra of ActD is noticed (data not shown), while for micellar bile salts concentrations a decrease of absorbance of ActD coupled with a splitting of the absorption maxima into two peaks and a bathochromic shift of these new absorption peaks (insets in Fig. 2) are observed. It can be observed that the addition of bile salts yields an isosbestic point at about 370 nm in the case of the interaction with NaC and at about 355 nm in the case of the interaction with NaDC. These spectral changes confirm the occurrence of interaction of ActD molecules with NaC and NaDC bile salts, which further indicates the new complex formation between drug molecules and bile salts. Also, the red shifts in the absorption maximum (insets in Fig. 2a and b) imply the transfer of ActD molecules from the aqueous solution into the bile salt assemblies with lower polarity.

The changes in the absorption maximum of ActD at 440 nm in the presence of varying bile salts concentrations were used to calculate the binding constant (K_b) and the partition coefficient (K_x), and the respective thermodynamic parameters, thus obtaining a quantitative characterization of the interaction between ActD and bile salt micelles.

The binding constant was determined using the Benesi–Hildebrand equation:²⁵

$$\frac{1}{A_0 - A} = \frac{1}{K_b(A_0 - A_1)c_{BS}} + \frac{1}{A_0 - A_1} \quad (2)$$

where c_{BS} is the concentration of bile salts, A_0 is the absorbance value in the absence of bile salts, A is the absorbance value in the presence of bile salts and A_1 is the absorbance value at infinite concentration of bile salts.

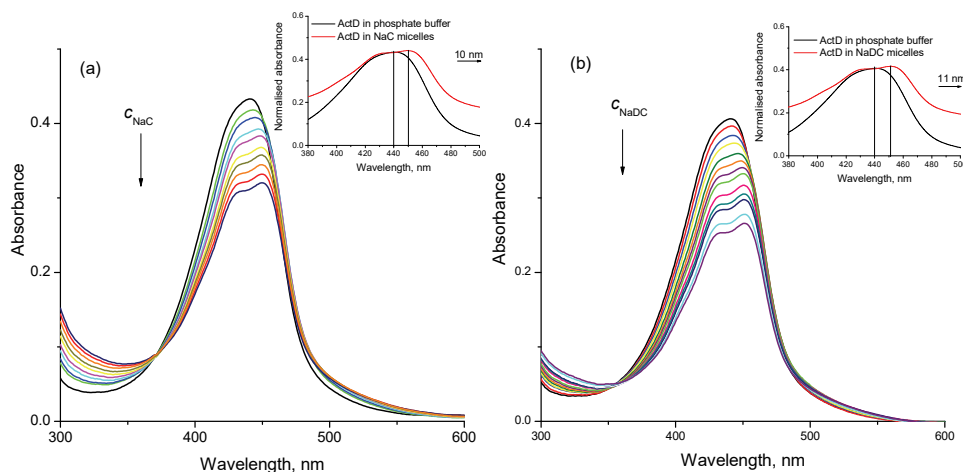


Fig. 2. Absorption spectra of ActD ($17.7 \mu\text{M}$) in 10 mM phosphate buffer (pH 7.4) with increasing concentration of bile salts: a) NaC (0–19.29 mM), b) NaDC (0–31 mM). Insets show the normalised absorption spectra of ActD in NaC and NaDC micelles.

The Benesi–Hildebrand plots of $1/(A_0 - A)$ versus $1/c_{\text{BS}}$ are shown in Fig. 3a and indicate a straight line for both bile salts which attest a 1:1 stoichiometric complexation between ActD and bile salts. The obtained binding constant values are listed in Table I and illustrate a stronger interaction of ActD with NaDC micelles than NaC micelles. The head groups of NaDC and NaC are the same ($-\text{COONa}$) but NaC contains one more hydroxyl group in its hydrophilic surface, making NaC less hydrophobic as compared to NaDC. The hydrophobicity index of NaDC and NaC are 0.72 and 0.13, respectively. Therefore, this difference in the hydrophobicity of NaC and NaDC leads to their distinct binding abilities and

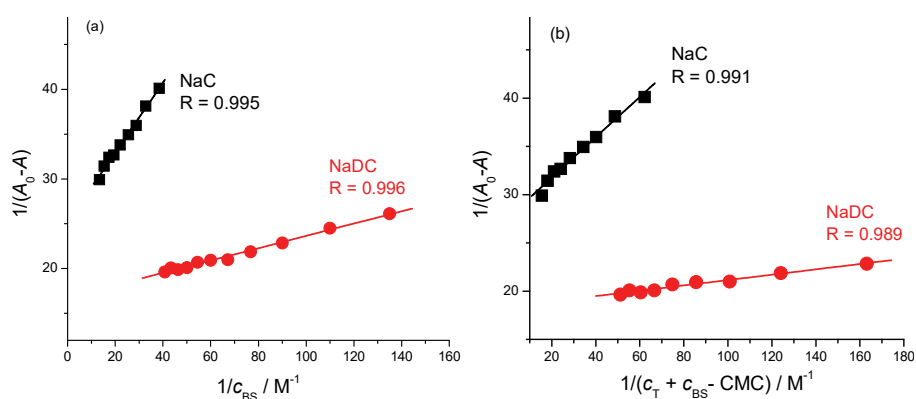


Fig. 3. a) Benesi–Hildebrand plots and b) Relation between $1/(A_0 - A)$ and $1/(c_T + c_{\text{BS}} - \text{CMC})$ for the interaction of ActD with NaC and NaDC micelles. R is the correlation coefficient.

prove that the hydrophobic interactions between ActD and NaDC micelles are much stronger compared to that between ActD and NaC micelles. The hydrophobic interactions between the planar aromatic chromophore of neutral ActD and the hydrophobic surface of bile salts are the main interaction forces responsible for the formation of ActD–bile salts complexes. Also, hydrogen bonds can be formed between the carbonyl oxygen atoms of the L-threonine residues of the pentapeptides chains of ActD and the hydroxyl groups of bile salts.

TABLE I. Binding constant (K_b), change in free energy of binding (ΔG_b^0), partition coefficient (K_x) and change in free energy of partition (ΔG_x^0) for the interaction of ActD with NaC and NaDC micelles

System	$K_b \pm SD^a / M^{-1}$	$\Delta G_b^0 / \text{kJ mol}^{-1}$	$K_x \pm SD^a$	$\Delta G_x^0 / \text{kJ mol}^{-1}$
ActD + NaC	68±5	-10.28	7294±187	-21.67
ActD + NaDC	281±12	-13.74	37822±2147	-25.68

^aStandard deviation of the mean of three determinations

The partition coefficient (K_x) was determined according to the pseudo-phase model:^{26,27}

$$\frac{1}{A_0 - A} = \frac{1}{A_0 - A_1} + \frac{n_w}{K_x(A_0 - A_1)(c_{BS} + c_T - CMC)} \quad (3)$$

In Eq. (3), c_T is the total ActD concentration and $n_w = 55.5 \text{ M}$ is the molarity of water.

The magnitude of partition coefficient (Table I) is very high for both bile salts and this result clearly suggests that the drug molecule resides into the hydrophobic environment of micelles rather than the aqueous medium. The partition coefficients value is significantly higher for NaDC micelles than NaC micelles, suggesting a larger affinity of ActD towards the more hydrophobic environment of NaDC. A larger degree of partitioning implies a greater number of ActD molecules accommodated into the hydrophobic core of NaDC micelles. Moreover, NaDC aggregates are known to be larger than the aggregates formed by NaC, as a consequence of the larger hydrophobic surface area²⁸ which supports the higher extent of partitioning of ActD molecules into NaDC aggregates. Both binding constant and partition coefficient parameters indicate that neutral ActD molecules are entrapped more efficiently into more hydrophobic core of NaDC aggregates than that of NaC aggregates. Studies performed by Thakur *et al.*¹⁷ showed that the neutral ellipticine is entrapped in the hydrophobic pocket of micellar aggregates of bile salts, while the cationic species are solubilized in the hydrophilic surface. The difference in the strength of binding and the partitioning of ActD molecules into NaC and NaDC aggregates can be explained by the differences in the micellar structures between dihydroxy and trihydroxy bile salts. Theoretical studies indicated that NaDC aggregates have a spherical structure

whereas NaC aggregates were disklike, oblate or flattened in shape and this difference is due to the various distributions in the hydrophilic moieties: for trihydroxyl bile salt NaC, the three hydroxyl groups and the headgroup form a plane of hydrophilic moieties whereas in the case of dihydroxyl bile salt NaDC, the hydrophilic groups are lined on the edge of the monomer.^{28,29}

From the values of K_b and K_x , change in free energy of interaction (ΔG_b^0) and change in free energy of the transfer of drug from bulk aqueous phase to micellar phase (ΔG_x^0) were calculated employing the following equation:

$$\Delta G^0 = -RT \ln K \quad (4)$$

The negative values of ΔG^0 for both binding and partitioning of ActD to NaC and NaDC micelles indicate the spontaneity and thermodynamic feasibility of both processes.

In order to obtain information about the possible positioning of ActD molecules into bile salts micelles we compared the absorption spectrum of the drug in surfactant micelles with the adsorption spectra in solvents with different polarities, which mimic the polarity of different parts of the micelles. Fig. 4 shows that the absorption spectra of ActD in 10 mM phosphate buffer present a broad maximum around 440 nm. In NaC and NaDC micelles, the absorption maximum of the drug is split into two peaks and these peaks are shifted to higher wavelength with about 10–11 nm. Also, it can be observed that the shape of ActD spectrum in solvents with different polarities is similar to the absorption spectrum in bile salts micelles, but the cleavage of the absorption maximum is more evident and the shift of the two newly appeared peaks towards longer wavelengths increases as the polarity of the solvents decreases. The absorption spectrum of ActD in NaC and NaDC micelles presents quite similar characteristics with the spectra in

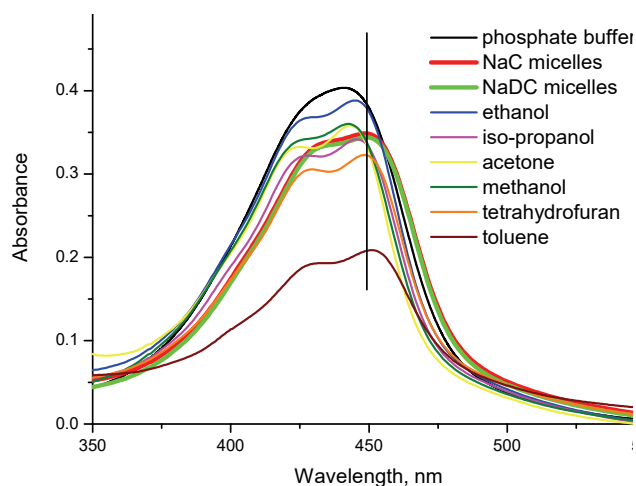


Fig. 4. Absorption spectra of ActD in different solvents and NaC and NaDC micelles.

non-polar solvents with dielectric constants smaller than 10 (tetrahydrofuran and toluene), thus we can say that ActD molecules are located in a hydrophobic microenvironment meaning that ActD molecules are more probable solubilized in the hydrophobic region, rather than in the hydrophilic region of micelles.

Determination of critical micellar concentration (CMC) of bile salts using pyrene probe

The UV spectral characteristics of pyrene in aqueous surfactant solutions are used for the estimation of *CMC* of cationic, ionic and nonionic surfactants.^{30,31} The absorption spectrum of pyrene in 10 mM phosphate buffer shows eight strong and weak peaks at 232, 240, 252, 260, 272, 308, 320 and 335 nm, as depicted in Figs. 5a and 6a. As the concentration of bile salts increases, pyrene molecules are incorporated in micelles and the absorption peaks of pyrene are shifted towards longer wavelengths and their intensities change. Plot of the sum of absorbances of all four major pyrene peaks (A_T) against the bile salts concentration is presented in Figs. 5b and 6b. The profiles show a sigmoidal increase and fitting them to the Sigmoidal–Boltzmann equation was used for *CMC* evaluation. Also, the absorbances of each major peak were also plotted separately and were all sigmoidal in nature. The obtained *CMC* values in 10 mM phosphate buffer (pH 7.4) are 0.0154 M for NaC and 0.0056 M for NaDC, respectively. These values are in the range of *CMC* values reported in literature and determined in water or in the presence of salt using other methods.^{32,33} The presence of ActD leads to the decrease of the *CMC* of NaC and NaDC bile salts. This decrease in *CMC* could be explained by the hydrophobic interactions between ActD

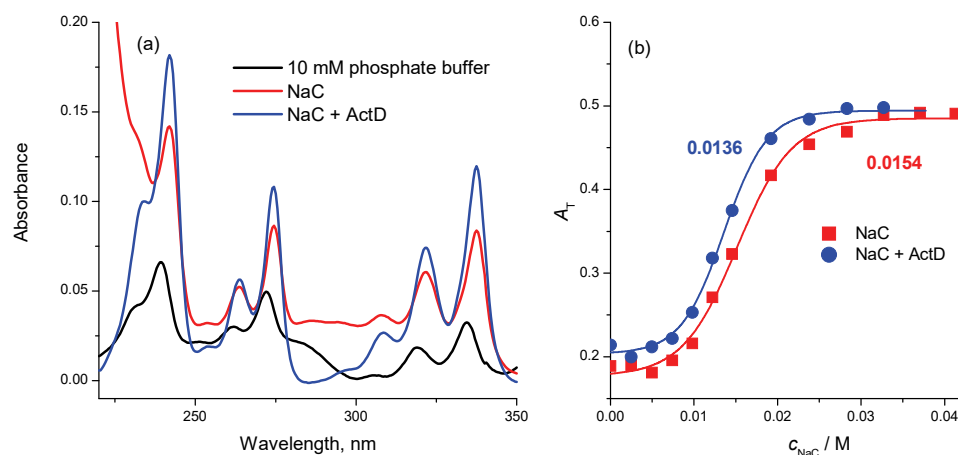


Fig. 5. a) Absorbance spectrum of pyrene (2.0 μM) in 10 mM phosphate buffer (pH 7.4), NaC micelles and NaC micelles in the presence of ActD. b) Plots of A_T vs. concentration of NaC. The values indicated on the graph are *CMC* of NaC and NaC in the presence of ActD.

and bile salts which further strengthen the hydrophobicity of studied bile salts and make their micellization process easier thereby lowering the CMC values.³⁴

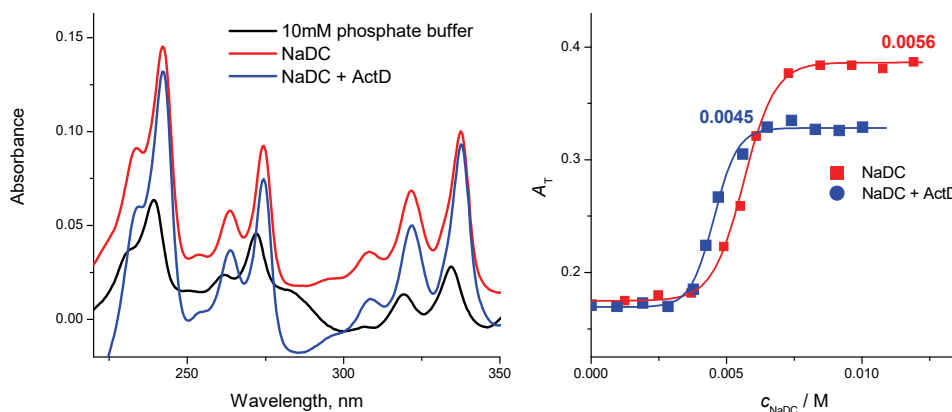


Fig. 6. a) Absorbance spectrum of pyrene (2.0 μ M) in 10 mM phosphate buffer (pH 7.4), NaDC micelles and NaDC micelles in the presence of ActD. b) Plots of A_T vs. c_{NaDC} . The values indicated on the graph are CMC of NaDC and NaDC in the presence of ActD.

Effect of NaC and NaDC micelles on ActD–DNA complex

Differing surfactant micelles,^{35–39} liposomes^{40,41} or surface active ionic liquids⁴² were studied for the effective sequestration of drugs after their deintercalation from DNA double helix. The binding of to DNA leads to an increase of melting temperature (T_m) of DNA of about 10 °C and this high positive value proves the intercalation binding mode of ActD to DNA. Also, the amplitude of the melting curve, which measures the hyperchromism of the system decreases (Fig. 7). When NaC and NaDC micelles are added to a pre-formed ActD–DNA

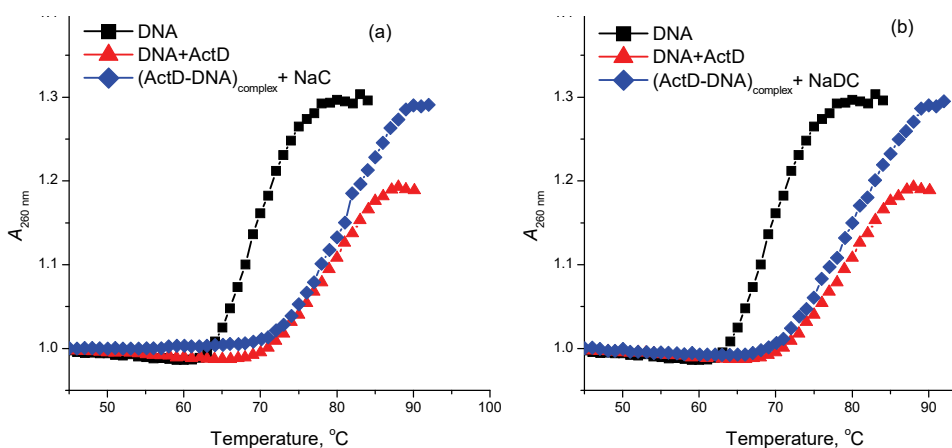


Fig. 7. Thermal melting profile of DNA, ActD–DNA complex and ActD–DNA complex in the presence of: a) NaC and b) NaDC micelles.

complex, the melting temperature does not change significantly (80.56 °C for NaC and 80.15 °C for NaDC as against 79.25 °C for ActD–DNA system), while the hyperchromicity increases almost up to the value corresponding to DNA alone (Table II). Also, the addition of NaC and NaDC micelles to ActD–DNA system induce minor changes (a small increase in absorbance in the case of NaDC micelles) in the absorption spectra (Fig. 8).

TABLE II. DNA melting temperature (T_m) and hyperchromicity (H) for DNA, ActD–DNA complex and ActD–DNA complex in the presence of NaC and NaDC micelles

System	$T_m / ^\circ\text{C}$	$H / \%$
DNA	69.58	23.04
ActD + DNA	79.25	15.97
ActD–DNA complex + NaC	80.56	22.94
ActD–DNA complex + NaDC	80.15	22.83

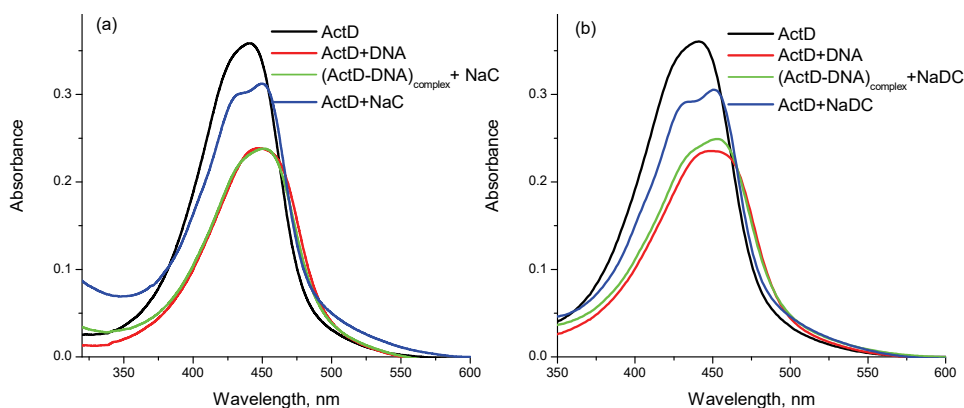


Fig. 8. Absorption spectra of ActD, ActD–DNA complex and ActD and ActD–DNA complex in the presence of: a) NaC and b) NaDC micelles.

These results show that the presence of NaC and NaDC micelles does not induce the deintercalation of ActD molecules from DNA duplex, probable due to the strong binding of ActD to DNA. In comparison with these results, the presence of SDS micelles induce the dissociation of the intercalated ActD molecules from DNA and their relocation in SDS micelles as was evidenced from spectral and thermal denaturation experiments.³⁹

CONCLUSIONS

The prominent changes observed in the absorption spectra (the decrease in absorbance, the red shift) of ActD in the presence of NaC and NaDC bile salts are clear statement of the interaction between drug molecules and bile salts, and the encapsulation of ActD molecules into the more hydrophobic environment provided by the bile salt aggregates. The results indicate that the binding cons-

tants and the partition coefficients are higher for NaDC aggregates and this difference can be explained by the difference in the micellar structure as well as the hydrophobicity of two bile salts. Regarding the position of ActD molecules into NaC and NaDC micelles, the spectral signatures of the drug in different solvents suggest that ActD molecule experiences the hydrophobic environment of bile salts micelles, rather than the hydrophilic medium. Considering the influence of NaC and NaDC micelles on the ActD–DNA complex, it was shown that the presence of both bile salts micelles does not induce the deintercalation of ActD molecules from DNA duplex.

ИЗВОД

ИНТЕРАКЦИЈЕ ВЕЗИВАЊА ЛЕКА АКТИНОМИЦИНА Д ПРОТИВ РАКА СА МИЦЕЛАМА ЖУЧНИХ СОЛИ

ANA MARIA TOADER, IZABELLA DASCALU, ELENA IONELA NEACSU и MIRELA ENACHE
*Institute of Physical Chemistry "Ilie Murgulescu", Romanian Academy, Splaiul Independentei 202,
Bucharest 060021, Romania*

Испитивана је интеракција лека актиномицина Д (ActD) против рака са две жучне соли различите хидрофобности: натријум-холат (NaC) и натријум-деоксихолат (NaDC), као и утицај агрегата ових жучних соли на комплекс између ActD и ДНК у 10 mM фосфатном пуферу (pH 7,4), користећи UV–Vis спектроскопске методе (апсорпције и термалне денатурације). Јаче је везивање ActD за NaDC него за NaC, што указује на јаче хидрофобне интеракције између ActD и NaDC мицела. Такође, коефицијент расподеле је значајно већи за NaDC него за NaC мицеле, што је у складу са формирањем већих агрегата NaDC. Профил спектра молекула ActD у NaC и NaDC мицелама, у поређењу са спектром у различитим растварачима, указује да је окружење ActD у мицелама жучних соли хидрофобно. Показано је и да мицеле ових жучне соли не изазивају деинтеркалацију молекула ActD из ДНК двоструког ланца, када се налази у комплексу ActD–ДНК.

(Примљено 2. новембра 2022, ревидирано 17. јануара, прихваћено 25. јануара 2023)

REFERENCES

1. J. C. Schink, D. K. Singh, A. W. Rademaker, D. S. Miller, J. R. Lurain, *Obstet. Gynecol.* **80** (1992) 817 ([https://doi.org/10.1016/0020-7292\(93\)90503-O](https://doi.org/10.1016/0020-7292(93)90503-O))
2. H. Hosoi, *Pediatr. Int.* **58** (2016) 81 (<https://doi.org/10.1111/ped.12867>)
3. R. D. Jenkin, R. D. Jeffs, C. A. Stephens, M. J. Sonley, *Can. Med. Assoc. J.* **115** (1976) 136 (<https://www.ncbi.nlm.nih.gov/pmc/articles/PMC1878570/pdf/canmedaj01484-0048.pdf>)
4. H. M. Sobell, *Proc. Natl. Acad. Sci. U.S.A.* **82** (1985) 5328 (<https://doi.org/10.1073/pnas.82.16.5328>)
5. A. F. Hofmann, L. R. Hagey, *Cell Mol. Life Sci.* **65** (2008) 2461 (<https://doi.org/10.1007/s00018-008-7568-6>)
6. J. Maldonado-Valderrama, P. Wilde, A. Macierzanka, A. Mackie, *Adv. Colloid Interface Sci.* **165** (2011) 36 (<https://doi.org/10.1016/j.cis.2010.12.002>)
7. Y. S. R. Elnaggar, *Int. J. Nanomedicine* **10** (2015) 3955 (<https://doi.org/10.2147/IJN.S82558>)

8. M. Stojancevic, N. Pavlovic, S. Golocorbin-Kon, M. Mikov, *Front. Life Sci.* **7** (2013) 112 (<https://doi.org/10.1080/21553769.2013.879925>)
9. C. Faustino, C. Serafim, P. Rijo, C. Pinto Reis, *Expert Opin. Drug Deliv.* **13** (2016) 1133 (<https://doi.org/10.1080/17425247.2016.1178233>)
10. D. Madenci, S. U. Egelhaaf, *Curr. Opin. Colloid Interface Sci.* **15** (2010) 109 (<https://doi.org/10.1016/j.cocis.2009.11.010>)
11. D. M. Small, S. A. Penkett, D. Chapman, *Biochim. Biophys. Acta* **176** (1969) 178 ([https://doi.org/10.1016/0005-2760\(69\)90086-1](https://doi.org/10.1016/0005-2760(69)90086-1))
12. D. M. Small, *Advances in Chemistry Series*, E. D. Goddard, Ed., Plenum Press, New York, 1968, p. 31 (<https://doi.org/10.1021/ba-1968-0084.ch004>)
13. S. Gouin, X. X. Zhu, *Langmuir* **14** (1998) 4025 (<https://doi.org/10.1021/la971155w>)
14. M. Posa, A. Sebenji, *Biochim. Biophys. Acta - Gen. Subj.* **1840** (2014) 1072 (<https://doi.org/10.1016/j.bbagen.2013.11.008>)
15. M. Haustein, P. Schiller, M. Wahab, H.-J. Mögel, *J. Sol. Chem.* **43** (2014) 1755
16. (<https://doi.org/10.1007/s10953-014-0239-3>)
17. M. Posa, A. Pilipovic, *J. Mol. Liq.* **238** (2017) 48 (<https://doi.org/10.1016/j.molliq.2017.04.109>)
18. R. Thakur, A. Das, C. Adhikari, A. Chakraborty, *Phys. Chem. Chem. Phys.* **16** (2014) 15681 (<https://doi.org/10.1039/C4CP01308E>)
19. S. Mandal, S. Ghosh, H. H. K. Aggala, C. Banerjee, V. G. Rao, N. Sarkar, *Langmuir* **29** (2013) 133 (<https://doi.org/10.1021/la304319r>)
20. S. Mandal, S. Ghosh, C. Banerjee, V. G. Rao, N. Sarkar, *J. Phys. Chem., B* **116** (2012) 8780 (<https://doi.org/10.1021/jp302435h>)
21. M. Gomez-Mendoza, E. Nuin, I. Andreu, M. Luisa Marin, M. A. Miranda, *J. Phys. Chem., B* **116** (2012) 10213 (<https://doi.org/10.1021/jp304708y>)
22. H. Nakazawa, N. R. Bachur, F. E. Chou, M. M. Mossoba, P. L. Gutierrez, *Biophys. Chem.* **21** (1985) 137 ([https://doi.org/10.1016/0301-4622\(85\)85015-8](https://doi.org/10.1016/0301-4622(85)85015-8))
23. R. Bittman, L. Blau, *Biochemistry* **14** (1975) 2138 (<https://doi.org/10.1021/bi00681a015>)
24. H. K. S. Souza, *Thermochim. Acta* **501** (2010) 1 (<https://doi.org/10.1016/j.tca.2009.12.012>)
25. H. E. Auer, *FEBS Lett.* **73** (1977) 167 ([https://doi.org/10.1016/0014-5793\(77\)80973-3](https://doi.org/10.1016/0014-5793(77)80973-3))
26. H. A. Benesi, J. H. Hildebrand, *J. Am. Chem. Soc.* **71** (1949) 2703 (<https://doi.org/10.1021/ja01176a030>)
27. L. Sepulveda, E. Lissi, F. Quina, *Adv. Colloid Int. Sci.* **25** (1986) 1 ([https://doi.org/10.1016/0001-8686\(86\)80001-X](https://doi.org/10.1016/0001-8686(86)80001-X))
28. H. Kawamura, M. Manabe, Y. Miyamoto, Y. Fujita, S. Tokunaga, *J. Phys. Chem.* **93** (1989) 5536 (<https://doi.org/10.1021/j100351a042>)
29. R. Li, E. Carpentier, E. D. Newell, L. M. Olague, E. Heafey, C. Yihwa, C. Bohne, *Langmuir* **25** (2009) 13800 (<https://doi.org/10.1021/la901826y>)
30. L. B. Partay, M. Sega. P. Jedlovsky, *Langmuir* **23** (2007) 12322 (<https://doi.org/10.1021/la701749u>)
31. G. B. Ray, I. Chakraborty, S. P. Moulik, *J. Colloid Interface Sci.* **294** (2006) 248 (<https://doi.org/10.1016/j.jcis.2005.07.006>)
32. L. Stopkova, J. Galisinova, Z. Suchtova, J. Cizmarik, F. Andriamainty, *Molecules* **23** (2018) (<https://doi.org/10.3390/molecules23051064>)
33. B. Natalini, R. Sardella, A. Gioiello, F. Ianni, A. Di Michele, M. Marinozzi, *J. Pharm. Biomed. Anal.* **87** (2014) 62 (<https://doi.org/10.1016/j.jpba.2013.06.029>)

34. T. S. Wiedmann, L. Kamel, *J. Pharm. Sci.* **91** (2002) 1743 (<https://doi.org/10.1002/jps.10158>)
35. K. Kumar, B. S. Patial, S. Chauhan, *J. Chem. Thermodyn.* **82** (2015) 25 (<http://dx.doi.org/10.1016/j.jct.2014.10.014>)
36. A. Mukherjee, S. Ghosh, M. Pal, B. Singh, *J. Mol. Liq.* **289** (2019) 111116 (<https://doi.org/10.1016/j.molliq.2019.111116>)
37. F. Westerlund, M. Wilhelmsson, B. Norden, P. Lincoln, *J. Am. Chem. Soc.* **125** (2003) 3773 (<https://doi.org/10.1021/ja029243c>)
38. A. Patra, S. Hazra, G. S. Kumar, R. K. Mitra, *J. Phys. Chem., B* **118** (2014) 901 (<https://doi.org/10.1021/jp4091816>)
39. M. Enache, S. Ionescu, E. Volanschi, *J. Mol. Liq.* **208** (2015) 333 (<https://doi.org/10.1016/j.molliq.2015.05.006>)
40. A. M. Toader, I. Dascalu, M. Enache, *Acta Chim. Slov.* **69** (2022) 331 (<https://dx.doi.org/10.17344/acsi.2021.7189>)
41. A. Das, C. Adhikari, D. Nayak, A. Chakraborty, *Langmuir* **32** (2016) 159 (<https://doi.org/10.1021/acs.langmuir.5b03702>)
42. A. Das, C. Adhikari, A. Chakraborty, *Langmuir* **32** (2016) 8889 (<https://doi.org/10.1021/acs.langmuir.6b01860>)
43. N. Maurya, Z. A. Parray, J. K. Maurya, A. Islam, R. Patel, *ACS Omega* **4** (2019) 21005 (<https://doi.org/10.1021/acsomega.9b02246>).